Journal of Basics and Applied Sciences Research (JOBASR)
ISSN (print): 3026-9091, ISSN (online): 1597-9962
Volume 3(1) January 2025
DOI: https://dx.doi.org/10.4314/jobasr.v3i1.2

# A Study on a Couette Flow of Conducting Fluid Heated/Cooled Asymmetrically

**Ibrahim, Y.[1*], Ahmad, N.[2], Idris, A.[3] and Musa, A. K.[4]**
[1, 2, 3]Department of Mathematics, Federal University Dutsin-Ma, Katsina State, Nigeria
[4]Department of Mathematics, Federal University Birnin Kebbi (FUBK), Nigeria
*Corresponding Author Email: yibrahim22@fudutsinma.edu.ng

**Keywords:**
Couette flow,
Buoyancy force ratio,
Conducting fluid.

**ABSTRACT**
This work presented a study on buoyancy force rate in couette conducting fluid flow. Quality of energy in the fluid flow problem was studied by the introduction of entropy. The mathematical model was transformed to non-dimensional form and solved using an analytical method of the regular perturbation technique in the absence of time. Various pertinent parameters with their effects on the velocity, temperature, entropy, volume flow rate was discussed and presented graphically. It is intriguing to observe that the findings of this study align with those of the anchor paper when the buoyancy force parameter is deactivated in the present work.

## INTRODUCTION

Thermal radiation plays a significant role in convective heat transfer processes which consist of high temperatures for example, gas turbines, solar power technology, and nuclear power plant. The impact of radiation on magnetohydrodynamic (MHD) flow and its vital role in the field of mechanical and thermal engineering such as storage thermal energy, chemical engineering, space vehicle re-entry, aeronautics, and electrical power generation, etc. in view of its significance, Isah and Jha (2015) examined the steady state natural convection flow in an annulus with thermal radiation, where they analyzed the interaction of fully developed natural convection flow with thermal radiation inside a vertical annulus. Isah et al (2018) discussed the thermal radiation effect on unsteady free-convective Couette flow of conducting fluid in the presence of transverse magnetic field. In this study, the model was highly non-linear due to the presence of thermal radiation. Combined effect of suction/injection on MHD free-convection flow in a vertical channel wit thermal radiation was studied by Isah et al (2018). A series of numerical experiments showed that time required reaching steady state velocity and temperature is directly proportional to the Prandtl number of the working fluid. Isah et al (2016) deliberated on combined effects of thermal diffusion and diffusion-thermo effects on transient MHD natural convection and mass transfer flow of viscous, incompressible and electrically conducting fluid between two infinite vertical plates in the presence of the transversal magnetic field, thermal radiation, thermal diffusion and diffusion-thermo effects was studied. Unsteady MHD free convective Couette flow between vertical porous plates with thermal radiation was investigated by Jha et al (2015). Significant result from this study are that both velocity and temperature increase with the increase in thermal radiation parameter and time. Lie et al (2018) studied control volume finite element method for nanofluid MHD natural convective flow inside a sinusoidal annulus under the impact of thermal radiation. This research proves that the inner surface temperature decreases with the augment of buoyancy forces. The impact of the linear/nonlinear radiation on incessantly moving thin needle in MHD quiescent Al-Cu/methanol hybrid nanofluid by Sulochana et al (2020). This work describes the periphery layer exploration of MHD (Magnetohydrodynamic) hybrid nanofluid (Al-Cu/methanol) flow besides an unceasingly moving needle submerged horizontally in the flow field. Narahari (2010) analyzed an unsteady free convection in Couette motion between two vertical parallel plates in the presence of thermal radiation where the moving plate is subject to constant heat flux and the plate at rest is isothermal.

All the above literatures consider MHD Linear/Nonlinear thermal radiation but did not consider heated/cooled asymmetric boundary condition. MHD natural convection flows, where devices are either heated or cooled have its wide applications in technological processes, such as the cooling of the core of a nuclear reactor in the case of power or pump failures and the warming and cooling of electronic components. Sing and Paul (2006) studied Transient Natural Convection between two vertical walls heated/cooled asymmetrically. Similarity solution of Laminar Natural Convection flow of Non-Newtonian

Visco-inelastic Fluids was studied by Pankaj et al(2016). Transient Natural Convection flow between vertical concentric cylinders heated/cooled asymmetrically by Jha and Oni (2018). Sarkar and Das (2012) studied Transient MHD Natural Convection between Two Vertical Walls heated/cooled asymmetrically. Gaur et al (2018) studied Transient free Convective Radiative flow between Vertical parallel plates heated/cooled asymmetrically with heat generation and slip condition. Effect of Induced magnetic field on natural convection in vertical concentric annuli heated/cooled asymmetrically was investigated by Kumar and Singh (2013). Kumar and Singh (2015) investigated the effects of induced magnetic field on natural convection with Newtonian heating/cooled in vertical concentric annuli.

In the above cited literatures, they consider heated/cooled asymmetric boundary condition but no single research considered MHD, Linear/Nonlinear thermal radiation. Keeping in mind, this current research work is board to extend the work of Isah et al (2018) by considering the influence of buoyancy force ratio parameter at the boundary. Some related research works were done by (Adamu et al. 2024, Hamza et al. 2024 and Ibrahim et al, 2024).

## MATERIALS AND METHODS

A steady natural convection Couette flow of a viscous, incompressible, electrically conducting and radiating fluid with buoyancy effects, entropy generation and heat fluxes separated between two infinite vertical parallel plates of a distance $H$ was considered. A strong homogeneous magnetic field $B_0$ is imposed normal to the plates in the presence of an induced radiative heat flux of intensity $q_r$, which is absorbed by the plate and transferred to the fluid. The Cartesian $(x', y')$ coordinate are taken with $x-axis$ along the moving plate in the upward direction and the $y-axis$ normal to it as shown in the figure 1.

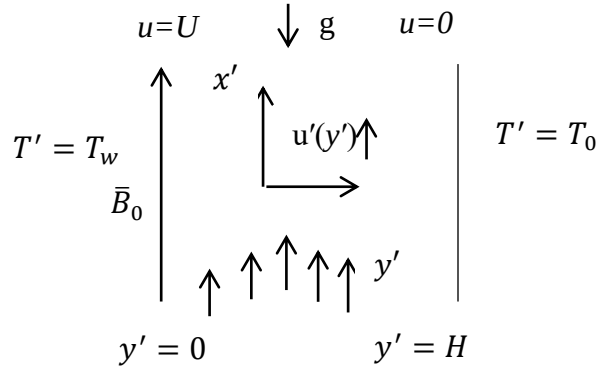


**Figure 1: Schematic diagram of the problem.**

The plates are infinite in length; the Momentum and Energy are functions of y alone. Using Boussinesq's approximation, the governing equations for the physical situation in dimensional form are:

Velocity Equation

$$\frac{\partial u'}{\partial t'} = \upsilon \frac{\partial^2 u'}{\partial y'^2} + g\beta\left(T' - T_m\right) - \frac{\sigma_1 B_0^2 u'}{\rho} \tag{1}$$

Temperature Equation

$$\frac{\partial T'}{\partial t'} = \alpha\left[\frac{\partial^2 T'}{\partial y'^2} - \frac{1}{K}\frac{\partial q_r}{\partial y'}\right] \tag{2}$$

The radiation heat flux term in the problem is simplified using the Roseland approximation

$$q_r = \frac{4\sigma \partial T'^4}{3\kappa^* \partial y'}$$

Where $\sigma$ and $\kappa^*$ are Stefan Boltzmann constant and Roseland mean absorption coefficient respectively.

The initial and boundary condition for the problem are

$$\left.\begin{aligned} t' \le 0 : u' = 0,\ T' = T_w\ \ 0 \le y' \le H \\ t' > 0 : u' = U,\ T' = T_w\ at\ y' = 0 \\ u' = 0,\ T' = T_0\ at\ y' = H \end{aligned}\right\} \tag{3}$$

Where $u', g, T', T_w, T_0, \rho, U\ and\ C_T$ are the fluid velocity, acceleration due to gravity, temperature of the fluid, temperature of the heated wall, temperature of the cooled wall, fluid density, velocity of the heated wall and temperature difference respectively.

To solve equation (1) and (2), we employ the following dimensionless variables and parameters.

$$\left.\begin{aligned} u = \frac{u'}{U},\ \theta = \frac{\left(T' - T_0\right)}{T_w - T_0},\ y = \frac{y'}{H},\ t = \frac{\upsilon t'}{H^2}, \\ r_t = \frac{\left(T - T_0\right)}{T_w - T_0},\ Gr = \frac{g\beta H^2\left(T_w - T_0\right)}{\nu U}, \\ R = \frac{4\sigma\left(T_w - T_0\right)}{K\kappa^*},\ C_T = \frac{T_0}{\left(T_w - T_0\right)}, \\ M^2 = \frac{\sigma_1 B_0^2 H^2}{\rho\nu},\ \Pr = \frac{\nu}{\alpha} \end{aligned}\right\} \tag{4}$$

The governing equations are transformed to the dimensionless form using equation (4) as follows:

Velocity Equation

$$\frac{\partial u}{\partial t} = \frac{\partial^2 u}{\partial y^2} + Gr\theta - M^2 u \tag{5}$$

Temperature Equation

$$\Pr\frac{\partial\theta}{\partial t}=\left[1+\frac{4R}{3}\left(C_T+\theta\right)^3\right]\frac{\partial^2\theta}{\partial y^2}+4R\left[C_T+\theta\right]^2\left(\frac{\partial\theta}{\partial y}\right)^2 \tag{6}$$

Subject to the following dimensionless initial and boundary conditions

$$\left.\begin{aligned} t\le 0: u=0,\ \theta=0\ \ for\ 0\le y\le 1\\ u=1,\ \theta=1\ at\ \ y=0\\ u=0,\ \theta=r_t\ \ at\ \ y=1\end{aligned}\right\} \tag{7}$$

**Method of Solution**

This section presents the governing system of non-linear coupled dimensionless partial differential equation of equation (5) and (6) subject to the boundary condition (7) by neglecting the time derivative.

Velocity Equation

$$0=\frac{d^2u}{dy^2}+Gr\theta-M^2u \tag{8}$$

Temperature Equation

$$0=\left[1+\frac{4R}{3}\left(C_T+\theta\right)^3\right]\frac{d^2\theta}{dy^2}+4R\left[C_T+\theta\right]^2\left(\frac{d\theta}{dy}\right)^2 \tag{9}$$

While the dimensionless initial and boundary conditions are:

$$\left.\begin{aligned} u=0,\ \theta=0\ \ for\ 0\le y\le 1\\ u=1,\ \theta=1\ at\ \ y=0\\ u=0,\ \theta=r_t\ \ at\ \ y=1\end{aligned}\right\} \tag{10}$$

In order to obtain approximate analytical solution of equations (8) and (9) subject to the boundary condition (10), a regular perturbation method will be employed by taking a power series expansion in the radiation parameter $R$ such as:

$$\left.\begin{aligned}\theta(y)=\theta_0(y)+R\theta_1(y)\\ u(y)=u_0(y)+Ru_1(y)\end{aligned}\right\} \tag{11}$$

Substituting equation (11) in (8) and (9) and equating the like powers of $R$ gives

$$u(y)=\frac{\sinh(My-M)}{M^2\sinh(M)}-\frac{(1+B_1)Gr}{M^2\sinh(M)}\sinh(My)+\frac{Gr}{M^2}+\frac{B_1Gr}{M^2}y+R\left[\left\{\left(\frac{8GrB_1^4}{M^6}+\frac{4GrB^2B_1^2}{M^4}\right)\frac{\sinh(M-My)}{\sinh(M)}\right\}+\frac{B_6}{\sinh(M)}\sinh(My)-\left\{\frac{8GrB_1^4}{M^6}+\frac{4GrB^2B_1^2}{M^4}\right\}+\left\{\frac{2GrB^2B_1^2}{M^2}+\frac{4GrBB_1^3}{3M^2}+\frac{GrB_1^4}{3M^2}-\frac{8GrBB_1^3}{M^4}\right\}y-\left\{\frac{4GrB_1^4}{M^4}+\frac{2GrB^2B_1^2}{M^2}\right\}y^2-\left\{\frac{4GrBB_1^3}{3M^2}\right\}y^3-\left\{\frac{GrB_1^4}{3M^2}\right\}y^4\right] \tag{12}$$

$$\theta(y)=\left\{A_0y+A_1\right\}+R\left[2B^2B_1^2\left(y-y^2\right)+\frac{4BB_1^3}{3}\left(y-y^3\right)+\frac{B_1^4}{3}\left(y-y^4\right)\right] \tag{13}$$

From (12), the steady-state skin frictions on the boundaries are:

$$\tau_0=\left.\frac{du}{dy}\right|_{y=0}=\frac{\left[1-Gr-B_1Gr\right]}{M\sinh(M)}+\frac{B_1Gr}{M^2}+R\left[\left\{\left(\frac{8GrB_1^4}{M^6}+\frac{4GrB^2B_1^2}{M^4}\right)\frac{(-M)}{\sinh(M)}\right\}+\left\{\frac{B_6M}{\sinh(M)}\right\}+\left\{\frac{2GrB^2B_1^2}{M^2}+\frac{4GrBB_1^3}{3M^2}+\frac{GrB_1^4}{3M^2}-\frac{8GrBB_1^3}{M^4}\right\}\right] \tag{14}$$

$$\tau_1=\left.\frac{du}{dy}\right|_{y=1}=\frac{\cosh(M)}{M\sinh(M)}-\frac{(1+B_1)Gr}{M\sinh(M)}\cosh(M)+\frac{B_1Gr}{M^2}+R\left[\left\{\left(\frac{8GrB_1^4}{M^6}+\frac{4GrB^2B_1^2}{M^4}\right)\frac{M\cosh(M)}{\sinh(M)}\right\}+\left\{\frac{MB_6\cosh(M)}{\sinh(M)}\right\}+\left\{\frac{2GrB^2B_1^2}{M^2}+\frac{4GrBB_1^3}{3M^2}+\frac{GrB_1^4}{3M^2}-\frac{8GrBB_1^3}{M^4}\right\}-\left\{\frac{8GrB_1^4}{M^4}+\frac{4GrB^2B_1^2}{M^2}\right\}-\left\{\frac{4GrBB_1^3}{M^2}\right\}-\left\{\frac{4GrB_1^4}{3M^2}\right\}\right] \tag{15}$$

Equally, from (13), the steady-state heat transfer on the boundaries are:

$$Nu_0 = -\left.\frac{d\theta}{dy}\right|_{y=0} = -A_0 - R\left[2B^2B_1^2 + \frac{4BB_1^3}{3} + \frac{B_1^4}{3}\right] \tag{16}$$

$$Nu_1 = -\left.\frac{d\theta}{dy}\right|_{y=1} = -A_0 - R\left[2B^2B_1^2 - 4B^2B_1^2 + \frac{4BB_1^3}{3} - 4BB_1^3 + \frac{B_1^4}{3} - \frac{4B_1^4}{3}\right] \tag{17}$$

## RESULTS AND DISCUSSION

In order to get the physical intuition of the flow parameters such as Buoyancy force rate $(r_t)$, Magnetic force $(M)$, Temperature difference $(C_T)$, Radiation parameter $(R)$ and Grashof number $(Gr)$ on the flow formation, a MATLAB software was used to compute and generate the graphs of the results. Fixed values selected

$$C_T = 0.01,\ M = 1.0,\ Gr = 1.0,\ R = 0.000001$$

**Velocity Profiles**

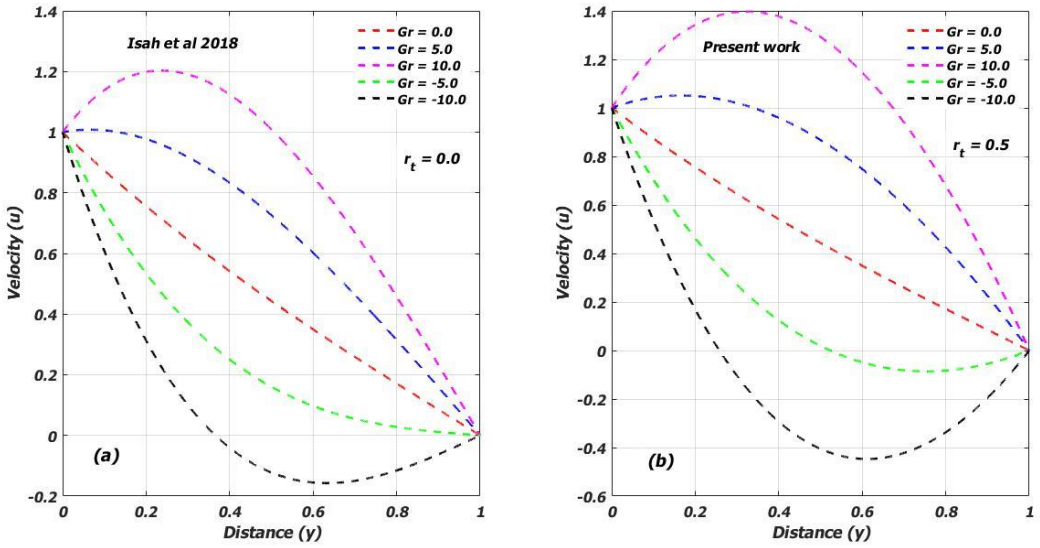


**Figure 2:** Comparison between Isah et al (2018) and present work on velocity profile with $R = 0.000001,\ C_T = 0.01\ and\ M = 1.0$

Figure 2(a) and (b) express the graphical representation of velocity profile for the present work and the benchmark paper respectively. Figure 2(a) agrees with Isah et al. (2018) where the same flow behavior has been observed with a difference in enhancement of the velocity in the present work which is due to the presence of buoyancy.

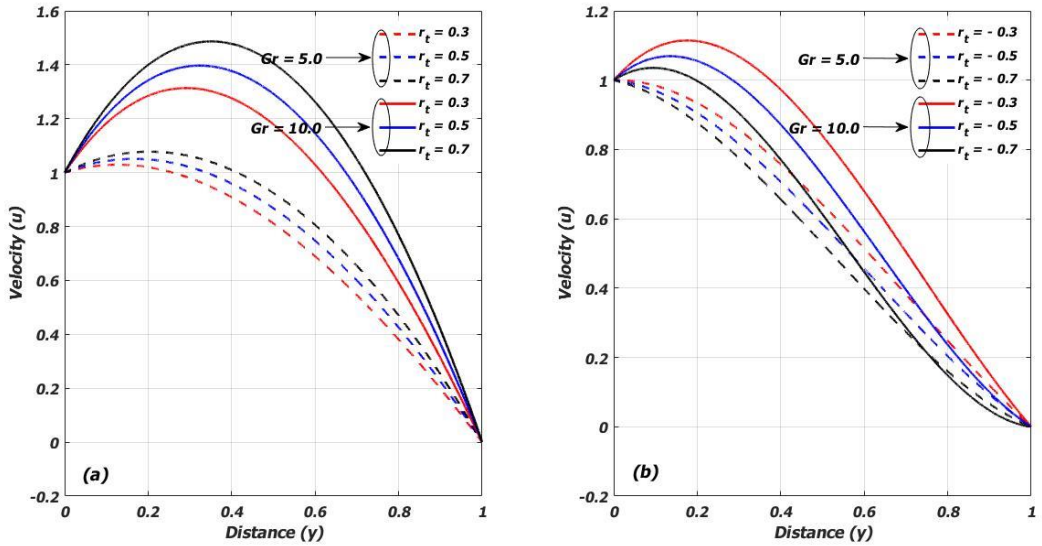


**Figure 3:** Effects of buoyancy force ratio $(r_t)$ and Grashof number $(Gr)$ on the velocity profile with $R = 0.000001,\ C_T = 0.01\ and\ M = 1.0$

Figure 3(a) and (b) demonstrate the velocity profiles for positive and negative values of buoyancy ratio $(r_t)$ respectively. Figure 3(a) exhibits the velocity profile for the case of . It is clear from the figure that the velocity is extreme near the heated wall $(T_w')$ and gradually decline towards the cooled wall $(T')$ due to the fairness between the temperature of the fluid $(T_0')$ and that of the cooled wall $(T')$, both which are less than the temperature of the heated wall $(T_w')$. The maximum velocity occurs in the middle $(y = 0.5)$ for $r_t = 0.7$ and it swings towards the wall $(y = 0)$ as $r_t$ varies from $0.7\ to\ 0.3$. This scenario transpires because for $r_t \geq 0.3$, the temperature of both walls $T_w'\ and\ T'$ is higher than the temperature of the fluid $(T_w')$. While for $r_t = 0.7$, the temperature of both walls $T_w'\ and\ T'$ is equal but greater than the temperature of the fluid $T_0'$.

The controlling parameter, $r_t$ acts as an enhancer between the heated $(T_w')$ wall and the cooled wall $(T')$ for making the nature of the flow to be parabolic. Figure 3(b) demonstrate the velocity profiles for the case of $r_t < 0.$ It can be observed that for $r_t = -0.3\ and\ -0.5,$ the reverse flow does not arise near the cooled $(T')$ wall but transpires for $r_t = -0.7$ as a result of more cooling of the flow. It can be seen that for $r_t < 0,$ the fluid temperature $(T_0')$ is higher than the temperature of the cooled wall $(T')$ but lower than the temperature of the heated wall $(T_0')$. As $r_t$ deviates from $-0.3\ to\ -0.7,$ the degree of the upward flow near the heated wall $(T_w')$ depreciates while the degree of the downward flow near the cooled wall $(T')$ appreciates.

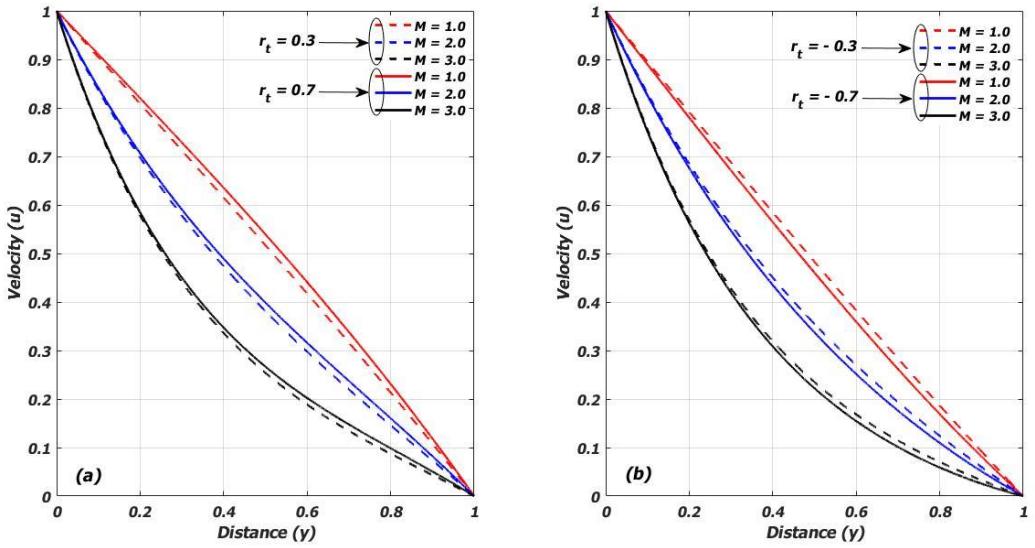


**Figure 4:** Effects of Magnetic force number $(M)$ on the velocity profile with $R = 0.000001$ *and* $C_T = 0.01$

Figure 4(a) and (b) show the effects Magnetic force (M) on the velocity profile. Figure 4(a) indicates that for positive values of the buoyancy force ratio parameter $(r_t)$, an increase in the Magnetic force (M) leads to the fall of velocity profile. This is because of the presence of transverse magnetic field which brings about the Lorentz force parameter (M) increase, so does the retarding force. However, velocity rises with higher value of $(r_t)$. Figure 4(b) shows that for $r_t < 0$, a rise in the magnetic force leads to the fall of the velocity profile.

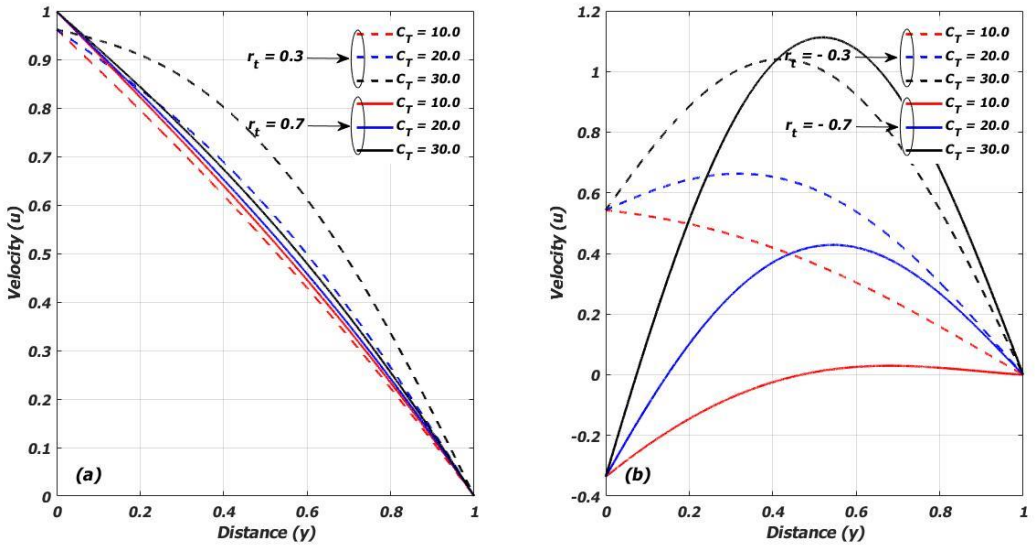


**Figure 5:** Effects of Temperature difference $(C_T)$ on the velocity profile with $M = 1.0$

Figure 5(a) and (b) depict the effects of temperature difference $(C_T)$ on the velocity profile. Figure 5(a) clearly shows that as the temperature difference $(C_T)$ and the buoyancy ratio $(r_t)$ increases, the fluid velocity also increases for the positive values of buoyancy ratio $(r_t > 0)$. The fluid velocity also increases for the positive values of buoyancy ratio $(r_t > 0)$. Figure 5(b) depicts the behavior of $C_T$ *for* $r_t < 0$. It can be

seen that for $C_T = 10,$ velocity decreases with high negative values of $r_t$. For $C_T = 20,$ the fluid velocity increases near the heated wall $\left(T_w^{'}\right)$. For $C_T = 30,$ the fluid velocity increases with high negative values of $r_t$.

**Temperature Profiles**

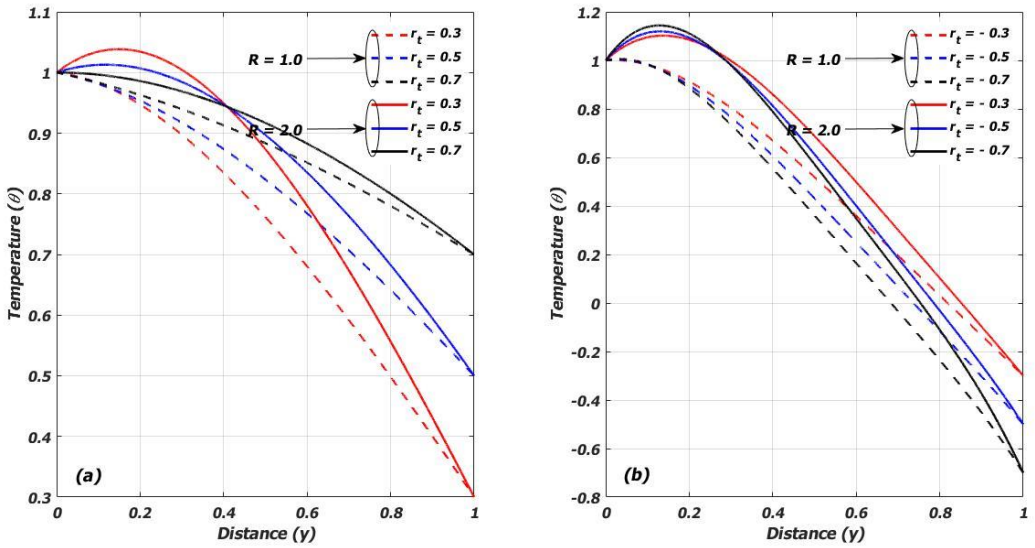


**Figure 6:** Effects of buoyancy force ratio $\left(r_t\right)$ on the temperature profile with $C_T = 0.01, Gr = 1.0 \; and \; M = 1.0$

Figure 6(a) and (b) depict the effects of buoyancy force ration $\left(r_t\right)$ on the temperature profile. Figure 6(a) clearly shows that for positive values of $r_t$, the temperature profile increases as the $\left(r_t\right) and \left(R\right)$ increase. The temperature appears to be slightly higher at the heated wall $\left(T_w^{'}\right)$ and twist at $\left(y = 0.41\right)$ towards the cooled wall $\left(T'\right)$. Figure 6(b) shows that for negative values of $r_t$, the temperature profile depreciates as $r_t$ increase but the temperature profile increase while (R) increase. The temperature of the fluid $\left(T_0^{'}\right)$ depreciates near the heated wall $\left(T_w^{'}\right)$ and twist at $\left(y = 0.25\right)$ towards the cooled wall $\left(T'\right)$. Temperature appreciates remarkably for $r_t < 0$ at the heated wall $\left(T_w^{'}\right)$ in comparison with $r_t > 0.$

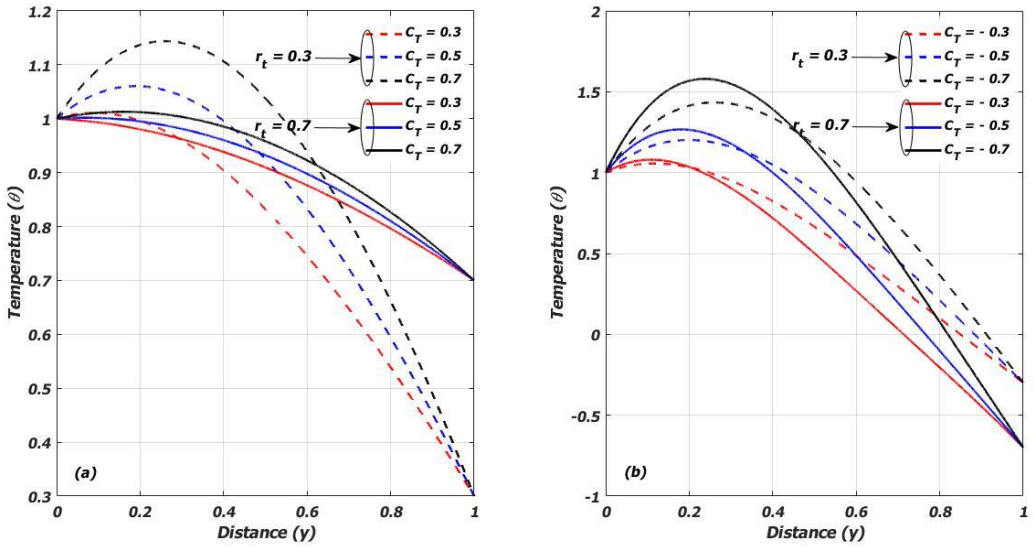


**Figure 7:** Effects of Temperature difference $(C_T)$ on the temperature profile with $M = 1.0$

Figure 7(a) and (b) show the effects of temperature difference $(C_T)$ on temperature profile. Figure 7(a) obviously shows that as the temperature difference parameter $(C_T)$ escalates, there is a corresponding rise in the temperature profile but falls with the increase in buoyancy ratio $(r_t)$. Figure 7(b) shows an increase temperature profile for high values of temperature difference $(C_T)$

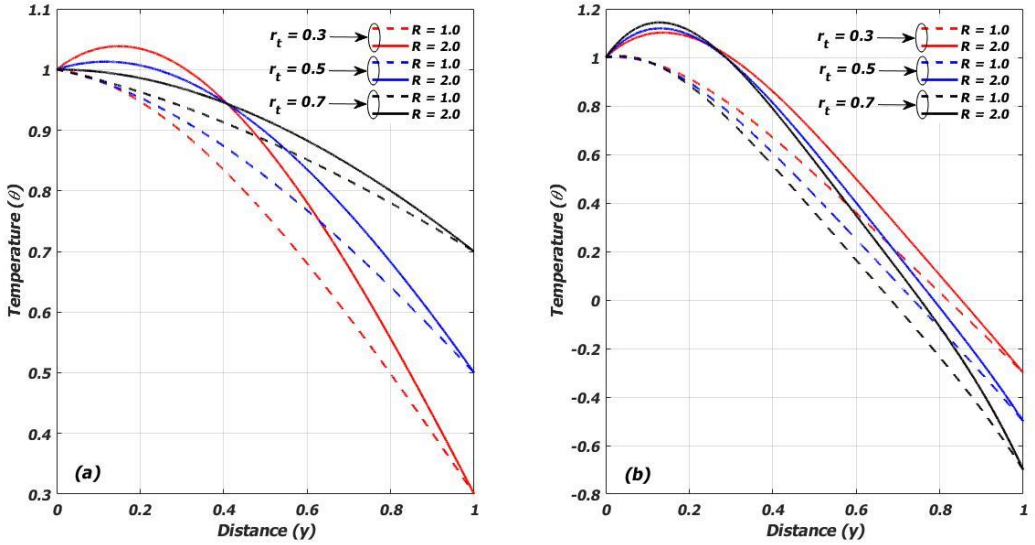


**Figure 8:** Effects of thermal radiation $(R)$ on the temperature profile with $C_T = 0.01$, $Gr = 1.0$ *and* $M = 1.0$

Figure 8(a) and (b) shows the effects of thermal radiation (R) on the temperature profile. Figure 8(a) shows that as radiation parameter (R) as well as the buoyancy ratio $(r_t)$ is improved, the temperature profile rises. This is because radiation is reliant upon temperature and higher values of radiation provide more heat to working fluid which appreciates the thermal condition of the fluid and its thermal boundary layer. Figure 8(b) represents the behavior of the temperature profile at different values of thermal radiation (R) with $r_t < 0$. The temperature profile is intensifying with greater values of thermal radiation (R) and buoyancy ratio parameter $(r_t)$ at the heated wall $(T_w')$ but decreases as it approaches the

cooled wall $(T')$. This proves that the heat is extreme at the heated wall $(T_w')$ than at the cooled wall $(T')$.

**Table 1:** Values of the skin friction at both walls in non-dimensional form

| $R$ | $r_t$ | $\tau_0$ | $\tau_1$ |
|---|---|---|---|
| 1 | 0.3 | 0.4087 | 0.6857 |
| 2 | | 0.4596 | 0.6144 |
| 3 | | 0.5105 | 2.5431 |
| 1 | 0.5 | 0.5122 | -0.0769 |
| 2 | | 0.6369 | 0.1517 |
| 3 | | 0.7615 | 0.3804 |
| 1 | 0.7 | 0.5092 | -0.3457 |
| 2 | | 0.6010 | -0.3232 |
| 3 | | 0.6928 | -0.3007 |

Table 1 showing the values of skin friction at both walls for different values of thermal radiation $(R)$ and buoyancy force ratio $(r_t)$ with a fixed values of $C_T = 0.01$ *and* $M = 1.$ An important observation from the table is that the values of the skin friction at both walls increases as the values of the buoyancy force $(r_t)$ increases. The values of $\tau_0$ are always greater than $\tau_1$ for other values of $r_t$ except at the initial stage. As the buoyancy force $r_t$ changes from 0.7 to 0.3, differences between the values of $\tau_0$ *and* $\tau_1$ increase, this suggests that a desired flow formation can be obtained by assigning a suitable value to the buoyancy force.

**Table 2: Values of the Nusselt number at both walls in non-dimensional form**

| $R$ | $r_t$ | $Nu_0$ | $Nu_1$ |
|---|---|---|---|
| 1 | 0.3 | -0.0822 | -1.0160 |
| 2 | | 0.5356 | -1.3320 |
| 3 | | 1.1535 | -1.6480 |
| 1 | 0.5 | -0.1375 | -0.7359 |
| 2 | | 0.2251 | -0.9718 |
| 3 | | 0.5877 | -1.2077 |
| 1 | 0.7 | -0.1500 | -0.4190 |
| 2 | | -0.4000e-05 | -0.5380 |
| 3 | | 0.1499 | -0.6570 |

Table 2 showing the values of Nusselt number at both walls for different values of thermal radiation $(R)$ and buoyancy force ratio $(r_t)$ with fixed values of $C_T = 0.01$ *and* $M = 1.$ Its observed from the table that the values of the Nusselt number at both walls increases as the value of the buoyancy force $(r_t)$ increases. It also shows that $Nu_0$ increases with increase in thermal radiation $(R)$, but decreases with increase in thermal radiation.

## CONCLUSION

A study on a couette flow of conduction fluid heated/cooled asymmetrically was studied. The results were discussed graphically for the pertinent parameters on the velocity and temperature, tables were also shown for the skin friction and Nusselt number. The result discloses that:

- The velocity and temperature are found to be appreciating for $r_t > 0.$ But the reverse is the case for $r_t < 0.$
- Values of the skin friction at both walls increases as the values of the buoyancy force $(r_t)$ increases.

- Values of the Nusselt number at both walls increases as the value of the buoyancy force $(r_t)$ increases.

The Grashof number enhances the fluid velocity.

And the following Recommendations have been made that the physical properties like density and thermal conductivity were considered to be constant, its however suggested for future research to vary these physical properties in order to accurately predict the flow and heat transfer rate.

**REFERENCE**

Adamu, A. A., Umar, I. T., Garba, I., Ibrahim, Y. (2024). Development and Energy Potential of Co-firing Fuel from Blends of Several Biomasses and Low Rank Coal at Optimal Condition. *Journal of Basics and Applied Sciences Research*, 2(3): 8-19.

Gaur, P. K., Sharma, R. P., and Jha, A. K. (2018). Transient free Convective Radiative Flow between Vertical parallel plates Heated/Cooled Asymmetrically with Heat Generation and Slip Condition. *Journal of Applied Fluid Mechanics*, 23(2): 365 – 384.

Hamza M. M., Isa M. M., Ibrahim Y., Usman H. (2024). Analysis of Magnetized Chemical Reaction under Arrhenius Control in the Presence of Navier Slip and Convective Boundary Conditions, *Journal of Basics and Applied Sciences Research*, 2(2): 71-82.

Ibrahim Y., Adamu I., Ibrahim U. T., Sa'adu A.Influence of Thermal Diffusion (Soret Term) on Heat and Mass Transfer Flow over a Vertical Channel with Magnetic Field Intensity. *Journal of Basics and Applied Sciences Research*, 2(2): 60-69.

Isah, B. Y., and Jha, B. K. (2015). Steady-State Natural Convection Flow in an Annulus with thermal Radiation, *Katsina Journal of Applied Mathematics*, 4(1): 8 – 21.

Isah, B. Y., Jha, B. K., and Lin, J. E. (2016). Combined Effects of Thermal Diffusion and Diffusion-Thermo Effects on Transient MHD Natural Convection and Mass Transfer Flow in a Vertical Channel with Thermal Radiation. *Applied Mathematics*, 7: 2354 – 2373.

Isah, B. Y., Jha, B. K., and Lin, J. E. (2018). On a Couette Flow of Conducting Fluid. *International Journal of Theoretical and Applied Mathematics*, 4(1): 8 – 21.

Isah, B. Y., Jha, B. K., and Uwanta, I. J. (2018). Combined effect of suction/injection on MHD free-convection flow in a Vertical channel with thermal Radiation. *Aim Shams Engineering Journal*, 9: 1069 – 1088.

Jha, B. K., and Oni, M. O. (2018). Transient Natural Convection Flow between Vertical Concentric Cylinders Heated/Cooled Asymmetrically. *J of Power and Energy* 12: 1 – 14.

Jha, B. K., Isah, B. Y., and Uwanta, I. J. (2015). Unsteady MHD free Convective Couette flow between vertical porous plates with Thermal Radiation. Journal of King Saud University-Science, 27: 338 – 348.

Kumar, A., and Singh, A. K. (2013). Effect of Induced Magnetic Field on Natural Convection in vertical Concentric Annuli Heated/Cooled Asymmetrically. *Journal of Applied Fluid Mechanics*, 6: 568 – 574.

Kumar, D., and Singh, A. K. (2015). Effect of Induced Magnetic Field on Natural Convection with Newtonian Heating/Cooling in vertical Concentric Annuli. *Procedia Engineering*, 127: 568 – 574.

Lie, Z., Sheikholeslami, M., Chamkha, A. J. Raizah, Z. A. F., and Saleem, S. (2018). Control Volume Finite Element Method for nanofluid MHD natural convective flow inside a sinusoidal annulus under the impact of Thermal Radiation. Computer Methods Applied Mechanical Engineering, 18: 25 – 35.

Nahari, M. (2010). Effects of Thermal Radiation and Free Convection Currents on the Unsteady Couette Flow between two Vertical Parallel Plates with Constant Heat Flux at one Boundary. *WSEAS Transactions on Heat and Mass Transfer*, 5(1): 1 – 11.

Panjak, S., Timol, M. G., and Salunke, J. N. (2016). Similarity Solution of Laminar Natural Convection Flow of Non-Newtonian Visco-inelastic Fluids. *International Journal of Innovative Science, Engineering and Technology*, 3(7): 2348 – 7968.

Sarkar, B. C. and Das, S. (2012). Transient MHD Natural Convection between two Vertical Walls Heated/Cooled Asymmetrically. *International Journal of Computer Applications*. 52(3): 27 – 34.

Singh, A., and Paul, T. (2006). Transient Natural Convection between two Vertical walls Heated/Cooled Asymmetrically. *International Journal of Applied Mechanics and Engineering.* 11(1): 143 - 154.

Sulochana, C., Aparna, S. R., and Sandeep, N. (2020). Impact of linear/nonlinear Radiation on incessantly moving thin needle in MHD Quiescent Al-Cu/methanol hybrid nanofluid. International Journal of Ambient Energy, 10: 1 – 21.